

RESEARCH ARTICLE

Structure, innervation and response properties of integumentary sensory organs in crocodilians

Duncan B. Leitch^{1,2} and Kenneth C. Catania^{2,*}

¹Neuroscience Graduate Program and ²Department of Biological Sciences, Vanderbilt University, Nashville, TN 37235, USA

*Author for correspondence (kenneth.catania@vanderbilt.edu)

SUMMARY

Integumentary sensory organs (ISOs) are densely distributed on the jaws of crocodilians and on body scales of members of the families Crocodylidae and Gavialidae. We examined the distribution, anatomy, innervation and response properties of ISOs on the face and body of crocodilians and documented related behaviors for an alligatorid (*Alligator mississippiensis*) and a crocodylid (*Crocodylus niloticus*). Each of the ISOs (roughly 4000 in *A. mississippiensis* and 9000 in *C. niloticus*) was innervated by networks of afferents supplying multiple different mechanoreceptors. Electrophysiological recordings from the trigeminal ganglion and peripheral nerves were made to isolate single-unit receptive fields and to test possible osmoreceptive and electroreceptive functions. Multiple small (<0.1 mm²) receptive fields, often from a single ISO, were recorded from the premaxilla, the rostral dentary, the gingivae and the distal digits. These responded to a median threshold of 0.08 mN. The less densely innervated caudal margins of the jaws had larger receptive fields (>100 mm²) and higher thresholds (13.725 mN). Rapidly adapting, slowly adapting type I and slowly adapting type II responses were identified based on neuronal responses. Several rapidly adapting units responded maximally to vibrations at 20–35 Hz, consistent with reports of the ISOs' role in detecting prey-generated water surface ripples. Despite crocodilians' armored bodies, the ISOs imparted a mechanical sensitivity exceeding that of primate fingertips. We conclude that crocodilian ISOs have diverse functions, including detection of water movements, indicating when to bite based on direct contact of pursued prey, and fine tactile discrimination of items held in the jaws.

Supplementary material available online at <http://jeb.biologists.org/cgi/content/full/215/23/4217/DC1>

Key words: brain, mechanosensory, trigeminal, behavior, touch, reptile, crocodile, alligator.

Received 28 June 2012; Accepted 23 August 2012

INTRODUCTION

Crocodilians' faces are covered in arrays of minute, pigmented skin elevations that are clearly visible around the upper and lower jaws. Early anatomical studies revealed differences in their distribution in the three families comprising Crocodylia (von Wettstein, 1937). In Alligatoridae, including the American alligator and caiman species, the protuberances are found only on the head near the mouth whereas in Crocodylidae and Gavialidae, they are found on virtually every scale of the body surface as well as on the head (Fig. 1). Despite their prominence, few studies have investigated their function. They have been hypothesized to play a role in secreting cleansing and waterproofing oils (Grigg and Gans, 1993), enabling osmoreception (Jackson and Brooks, 2007; Jackson et al., 1996), mediating mechanotransduction (Necker, 1974) and facilitating courtship behavior (Brazaitis and Watanabe, 2011). Other suggestions include possibly acting as electroreceptors, as a consequence of the aquatic habitat of crocodilians (Bullock, 1999), or acting as magnetoreceptors, an ability noted in alligators (Rodda, 1984). More recently, Soares (Soares, 2002) discovered that these structures in juvenile *Alligator mississippiensis* mediate an orienting response to the center of a water surface disturbance. As a result, it was proposed that the main role of these structures is the detection of surface waves generated by prey moving in water, and they were termed 'dome pressure receptors' [these organs have been given a variety of names in different studies – we have chosen to follow the functionally neutral and commonly used term 'integumentary

sensory organ' (ISO) (Brazaitis, 1987)]. Although detection of water disturbances is clearly useful to crocodilians, a number of observations suggest that ISOs could facilitate a wider array of mechanosensory abilities. For example, the ISOs of crocodylids are found across their entire body and are thus poorly situated for receiving surface waves. In alligators, the highest densities of ISOs are found around the teeth, inside the mouth, and at the rostral margins of the mandibles and maxilla, suggesting a role in discriminating food items or determining appropriate bite force (Erickson et al., 2012). Reflecting this uncertainty regarding their functions, these receptors have also been identified as 'integumentary osmoreceptors' in respect to the body receptors found in crocodylids (Jackson and Brooks, 2007).

The goal of this study was to provide further insight into the function of the ISOs by comparing them across two species of crocodilians: the Nile crocodile (*Crocodylus niloticus*) and the American alligator (*A. mississippiensis*). Here we examine the anatomy of ISOs, the branching patterns of afferents providing innervation and the physiological response properties of afferents from the skin areas covered with ISOs, and document some behaviors of alligators and crocodiles capturing prey under infrared illumination and with white noise to mask audition. Our results suggest that both the cranial and body ISOs of juvenile crocodilians are employed as a high-resolution mechanosensory system that allows for an otherwise armored skin surface to have a sensitivity greater than primate fingertips.

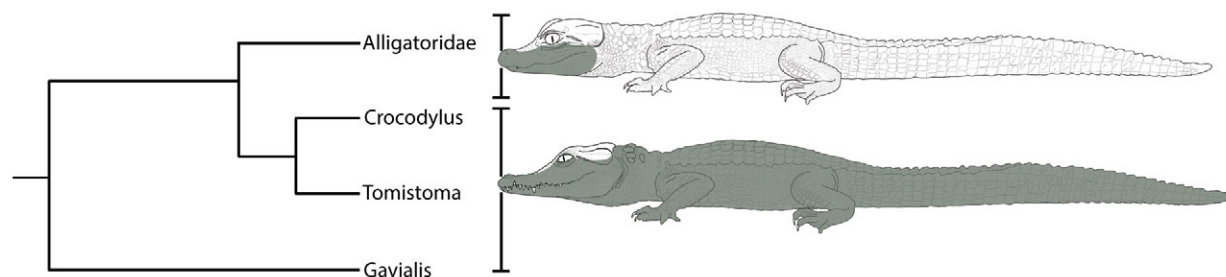


Fig. 1. The phylogeny of extant crocodilians, as modified from Brochu (Brochu, 2003). The distribution of integumentary sensory organs (ISOs) is indicated by the shaded regions. Within the order Alligatoridae, which includes all *Caiman* and *Alligator* species, ISOs are restricted to cranial regions. Within the *Crocodylus*, *Tomistoma* and *Gavialis* genera, ISOs are located on the cranium as well as along the rest of the post-cranial integument. Debate continues on the phylogenetic relationship of *Tomistoma* to *Gavialis*, depending on the genomic materials used in analysis (Piras et al., 2010).

MATERIALS AND METHODS

Animals

Eighteen American alligators (*Alligator mississippiensis* Daudin 1801) and four Nile crocodiles (*Crocodylus niloticus* Laurenti 1768) were studied. The alligators were provided by the Louisiana Department of Wildlife and Fisheries and were from the Rockefeller Wildlife Refuge (Grand Chenier, LA, USA), and Nile crocodiles were purchased from a commercial reptile breeder (Brooksville, FL, USA). They ranged in total body length from 15 to 92 cm and in mass from 30 g to 3.2 kg (from newly hatched to ~3 years old).

Scanning electron microscopy

Animals used to examine external skin structures were killed with sodium pentobarbital (120 mg kg^{-1}) and perfused with 4% paraformaldehyde (PFA). Tissues from the head and body surface were immersion fixed for 24 to 48 h, rinsed with phosphate-buffered saline (PBS), and dehydrated in a graded series of ethanol. Following dehydration, samples were critically point dried in an E3000 drier (Quorum Technologies, Guelph, ON, Canada) and coated with gold in a Cressington 108 sputter coater (Cressington Scientific Instruments, Watford, UK). Specimens were imaged using a Tescan Vega II SEM (Tescan, Cranberry Twp, PA, USA).

Sudan Black B

Specimens were fixed in 4% PFA for at least 1 week, washed in tap water for 12 h and then cleared in 10% hydrogen peroxide for 2 to 3 days. Following washes in deionized water, maceration in trypsin solution and washing in potassium hydroxide, the samples were stained in Sudan Black B solution (0.5 g Sudan Black B, Sigma-Aldrich, St Louis, MO, USA). Specimens were destained in ethanol and preserved in glycerin.

Receptor density measurements

Surfaces of the heads from two alligators [snout-vent length (SVL)=46 cm] were photographed by incrementally rotating the samples. Individual photographs were aligned based on distinguishing landmarks to create a complete montage of the scaled surfaces of the dorsal and ventral surfaces of the upper and lower jaws, and inside the oral cavity. A grid of 36 squares, each $2 \times 2 \text{ mm}$, was superimposed on the completed montages. The number of receptors within each box was counted, excluding the top and left walls, and the distance between individual receptors was measured using ImageJ (National Institutes of Health, Bethesda, MD, USA). Results from the four hemispheres were averaged.

Dil and confocal microscopy

Scale surface samples were removed post-mortem from PFA-fixed tissues. Small crystals of DiI (1,1'-dioctadecyl-3,3,3',3'-tetramethylindocarbocyanine perchlorate; Molecular Probes, Invitrogen, Carlsbad, CA, USA) were applied with insect pins to the exposed branches of the maxillary and mandibular nerves innervating facial regions and to the intercostal nerves for the ventral body surface. The scales were embedded in 2% agarose, immersed in 4% PFA and stored in darkness for ~1 week. The specimens were sectioned sagittally on a Vibratome Series 1000 (Technical Products International, St Louis, MO, USA) and imaged on an upright LSM510 confocal microscope (Zeiss, Thornwood, NY, USA).

Trigeminal nerve light microscopy

Segments of the ophthalmic, maxillary and mandibular branches of the trigeminal nerve from three age-matched yearling alligators and two Nile crocodiles, ~2 years old, were dissected following perfusions with 4% PFA. Tissue was sampled 2 to 4 mm from the body of the trigeminal ganglion, and specimens were immersed in phosphate-buffered 2.5% glutaraldehyde solution for least 24 h. Samples were post-fixed in osmium tetroxide, dehydrated in a graded ethanol series, transferred into propylene oxide and embedded in EMBED 812 (EM Sciences, Hatfield, PA, USA). Samples were sectioned transversely at $\sim 0.5 \mu\text{m}$ thickness using a diamond knife (Diatome US, Hatfield, PA, USA) on a Reichert Ultracut E ultramicrotome (Leica Microsystems, Wetzlar, Germany). Tissue was examined at $100\times$ under light microscopy (Zeiss Axioskop, Zeiss, Jena, Germany), and digital images were captured (Axiovision 4.5, Zeiss) and compiled in Adobe Photoshop CS5 (Adobe Systems, San Jose, CA, USA) into complete montages of the transverse section of the nerve of interest. Myelinated axons were manually counted.

Trigeminal and peripheral responses

Eighteen alligators and two Nile crocodiles were anesthetized with a combination of urethane (0.4 g kg^{-1}), ketamine (100 mg kg^{-1}) and xylazine (20 mg kg^{-1}). Supplemental doses were given as needed. The trigeminal ganglion ipsilateral to the stimulated body surface was exposed. For recordings from the body integument, the radial and ulnar nerves were exposed in the proximal regions of the forelimb, and the median nerve was exposed in the hindlimb. Receptive fields were marked on photographs of the body. Multi-unit and single-unit electrode recordings were made ~ 400 to $800 \mu\text{m}$ from the ganglion's surface using tungsten electrodes (1.0 to $1.5 \text{ M}\Omega$ at 1000 Hz). Responses were collected using a Bak headstage and preamplifier (BAK Electronics, Mt Airy, MD, USA) and sent

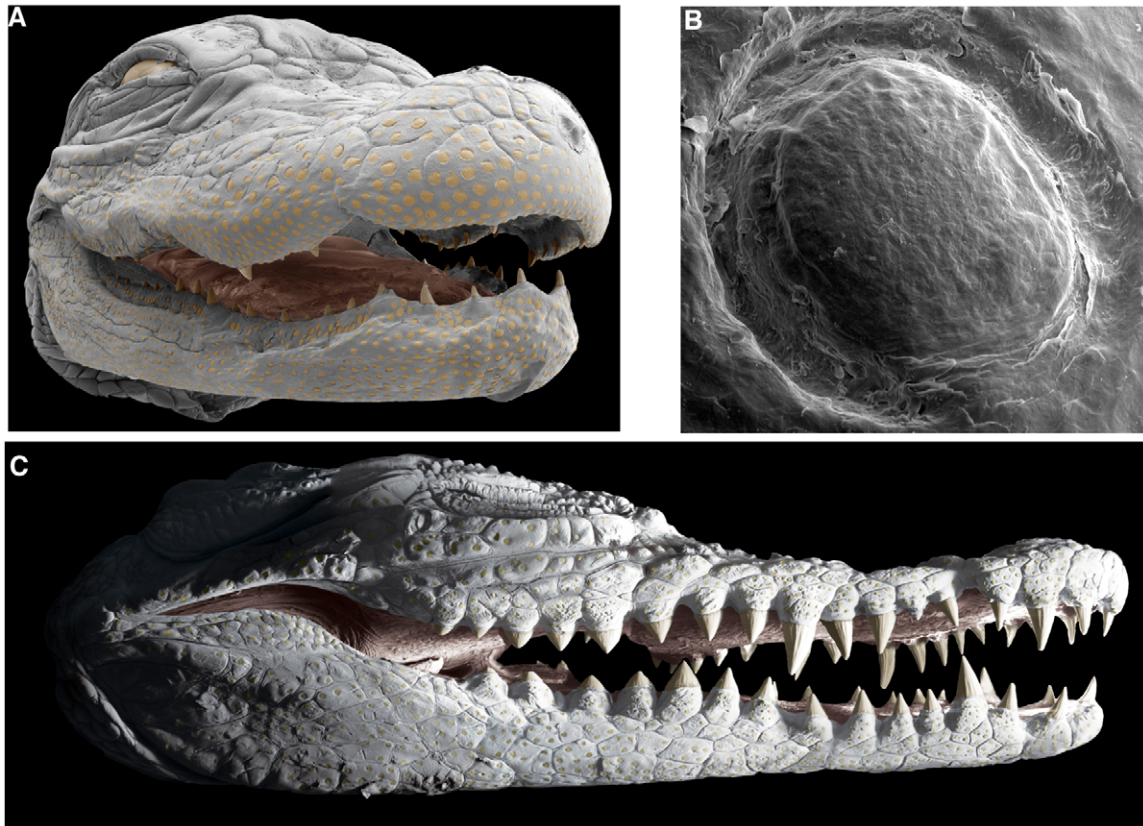


Fig. 2. Crocodilian cranial regions viewed under the scanning electron microscope. (A) The colorized head of an *Alligator mississippiensis* hatchling. The ISOs (yellow) are visible as circular, dome-shaped elevations. (B) A single *A. mississippiensis* ISO is shown at higher magnification, with a hinge region surrounding the elevated central region of the ISO. (C) The cranial regions from a *Crocodylus niloticus* juvenile, showing the distribution of ISOs.

to a Neurolog amplifier and filters (Digitimer, Welwyn Garden City, Herts, UK). Responses were monitored using speakers and waveforms from single units were collected at $100,000 \text{ samples s}^{-1}$ using LabChart 7.0 software using a PowerLab 4/30 system (ADInstruments, Colorado Springs, CO, USA) attached to a MacBook laptop (Apple, Cupertino, CA, USA). The skin surface was kept moist during recordings.

Several combinations of somatosensory stimuli were used to elicit responses from the skin surface. Scales were examined with small wooden probes and von Frey filaments (Stoelting Company, Wood Dale, IL, USA). Filaments just beyond threshold for eliciting a response were used in detailing the borders of receptive fields on photographs of the skin surface. Using the Chubbuck stimulator (Chubbuck, 1966) and the digital sine and square wave generator in LabChart 7.0, the frequency of the tactile stimuli was systemically altered. The motion of the stimulator was recorded to observe the timing of responses. Other stimuli included various positions of a pair of 9 V batteries and room-temperature hypertonic salt solutions (47 p.p.t. or greater) using Instant Ocean sea salts (Aquarium Systems, Mentor, OH, USA).

Following recordings, selected trigeminal ganglion electrode penetrations were lesioned with a $10 \mu\text{A}$ current for 15 s while the electrode was withdrawn from the ganglion at $50 \mu\text{ms}^{-1}$; other selected penetrations were marked with Toluidine Blue stain. Crocodilians were given an overdose of pentobarbital and perfused with PFA, as described above. Images of the intact ganglion were matched with photographs marked with locations of electrode penetrations. The results from six alligators' trigeminal ganglia were

used to reconstruct the somatotopy of the ganglion. Measurements of receptive field size were made using ImageJ.

Single-unit recordings ($N=110$) from four alligators' trigeminal ganglia were used to assess characteristics of receptor-covered skin. Data collected through LabChart 7.0 were analyzed using the Spike Histogram module to measure the interspike interval between consecutive action potentials. This was measured in the static phase (200 to 500 ms) after the dynamic response to initial stimulus presentation.

To assess differences between the von Frey force thresholds, the surface area of receptive fields and the location of the field (from either crocodile or alligator and from the cranial or post-cranial body scales from both), a series of independently sampled t -tests was run. Pearson correlation coefficients and Spearman's rank correlation coefficients were calculated, as the force thresholds represented a discontinuous data set whereas receptive field surface areas were continuous. All statistical analyses were two-tailed and set at the 0.05 level of significance. These were completed using JMP Version 9.0 (SAS Institute, Cary, NC, USA).

Behavior

Nile crocodiles and American alligators were filmed with a MotionPro HS-3 camera with video recorded on a MacBook Pro computer running MotionProX software (Redlake, Integrated Design Tools, Tallahassee, FL, USA). Animals were placed in aquaria with room-temperature water and permitted to move freely. Infrared (IR) lighting was provided on indicated trials with two IR-Flood Ultra-Covert 940 nm illuminators (Night Vision Experts, Buffalo, NY,

USA). White noise was presented on indicated trials as generated in Audacity (Carnegie Mellon Computer Music Group, Pittsburgh, PA, USA). Video was analyzed using iMovie (Apple). All procedures conformed to the National Institutes of Health standards concerning the use and welfare of experimental animals and were approved by the Vanderbilt University Animal Care and Use Committee.

RESULTS

In examining the crocodilian ISOs, several levels of analysis were adopted for both alligatorids and crocodylids. These data begin with describing the distribution of the organs, then their structure and innervation, and next, the trigeminal and spinal afferent electrophysiological responses recorded from the stimulation of skin and individual ISOs. Finally, some behavioral observations of the animals orienting towards food pellets and live prey are noted in reference to supplementary material Movie 1.

ISO distribution

Fig. 2A shows the head of a juvenile American alligator. Skin on the dorsal and ventral areas was covered in small, elevated sensory organs (Fig. 2B). In each of the three juvenile alligators examined, which included a single 1-year-old alligator (head length=7.2 cm) and two ~3-year-old alligators (head length=15.0 cm), there were 4200 ± 94 ISOs (mean \pm s.d.) distributed across the cranial regions. In the same areas on two juvenile Nile crocodiles (Fig. 2C), there were 3001 and 2811 ISOs. These cranial ISOs varied in size across the facial surface, with the smallest receptors found in apposition to and between the teeth and the largest receptors located on the dorsal surface of the maxilla, with mean diameters of 0.2 ± 0.03 to 1.2 ± 0.04 mm, respectively. Within the oral cavity, the ISOs were distributed across the upper palate and the gingivae near the tongue. In alligators, the greatest concentration of ISOs (>2.00 receptors mm^{-2} on a 15 cm head) was surrounding the teeth, and lower densities were found on the dorsal maxilla (Fig. 3). The distance between ISOs ranged from 0.3 ± 0.09 mm in the areas surrounding the incisor teeth on the rostral dentary to 4.9 ± 0.13 mm on the dorsal surface of the maxilla. For the anterior–posterior axis, ISO density was greater near the most anterior point, particularly on the lower jaw. Interestingly, disjunct areas of greater ISO density were found directly ventral to the eye and surrounding the nares. No evidence was found for other receptor organs (e.g. ampullary organs, ciliated receptors).

The post-cranial receptors of crocodylids were less densely distributed but found across the entire integument, including on the armored post-nuchal scales and osteoderms on the dorsal surface. Similar to the cranial receptors, they were visible as small, pigmented protuberances; however, there was typically only one ISO located caudally on each scale (occasionally as many as two to three). As a result, they were densest where the scales themselves were small, most notably near the cloaca.

ISO structure and innervation

Below the outer keratinized layers of epidermis of each ISO, a diversity of mechanoreceptors was positioned just beneath the stratum spinosum, supplied by a network of myelinated and unmyelinated axons. Transverse sections from the receptor revealed a number of anatomically distinct endings of the innervating axons (Fig. 4). The connective tissue below each receptor contained many melanocytes and provided the ISOs with their distinctive pigmentation. Just below the stratum basale, the melanocytes branched extensively and were filled with darkly colored melanin

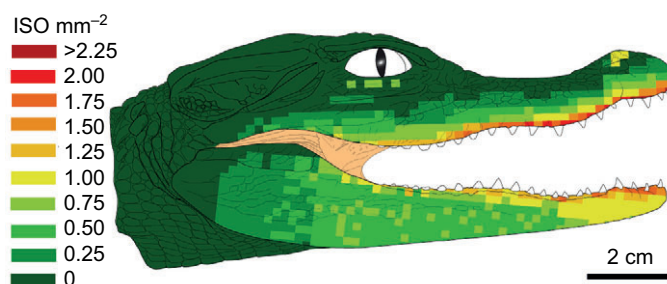


Fig. 3. Density of the ISOs across the cranium of a juvenile *A. mississippiensis*. Density was greatest directly adjacent to the teeth and near the rostral-most points of the maxilla and dentary. Isolated patches of greater density were found surrounding the nares and below the eye.

granules. These granules were interspersed with the mechanoreceptors. Unmyelinated free nerve endings, $\sim 0.5 \pm 0.09$ μm in diameter, passed through the connective tissue layers and terminated in the outer stratum spinosum. Branching from larger bundles of myelinated axons, free intraepidermal terminals were visible as ubiquitous 'discoid receptors' and could be distinguished based on their rounded, expanded structure located just below the cells of the stratum lucidum and corneum. Discoid receptors were closely coupled to the tonofibrillar structures of the adjacent cells of the spinosum and lucidum, and fluorescent, lipophilic dye applied to the proximal ends of the myelinated bundles often labeled the keratinized cells of the stratum corneum. The extracellular space between individual stratum spinosum cells was compressed at the point of receptor termination where the discoid receptors were located and surrounded by the tonofibrils of individual neighboring cells. Reflecting this compression, the keratinized layers of the stratified epithelium directly over the ISOs were $\sim 60\%$ thinner than that of adjacent scaled regions ($N=24$, mean= 61 μm , s.d.= 27 μm). The most superficial of the keratinized layers, the stratum corneum, appeared thinnest in the domed receptor region and at the hinged region of epidermal folds between individual scales.

Within the connective tissue beneath each receptor, numerous axon terminals were ensheathed in lamellations of Schwann cell processes (Fig. 4C). They appeared similar to the Paciniform corpuscles found in mammalian skin (Pease and Quilliam, 1957). There were also mechanoreceptor components that were not affiliated with Schwann cell elaborations. These included free axon terminals running parallel to the collagen fibers and ending in the dermis, with the morphology of previously identified branched lanceolate terminals (von Düring and Miller, 1979).

The most prominent sensory nerve endings of the ISOs were associated with the dermal Merkel cell column, located below the center of the dome and the surrounding stratum spinosum, where many of the axons traversing the longitudinal axis between domes converged (Fig. 4D). A similar configuration has been described in *Caiman* (von Düring, 1974). This structure was easily distinguished as a mass of elongated, flattened Merkel cells with intercalated axon terminals and was distinct in its limited distribution to regions under the ISOs.

The ISOs were supplied by fibers that originated below the superficial layers of the collagenous tissue from an elaborate network of myelinated fibers that ran parallel to the skin surface. These branched most distally at the dome receptor regions into fascicles that typically contained 15 or more myelinated axons (Fig. 4B, arrows). At more superficial levels, these branches coursed together in circular patterns, ringing the inner

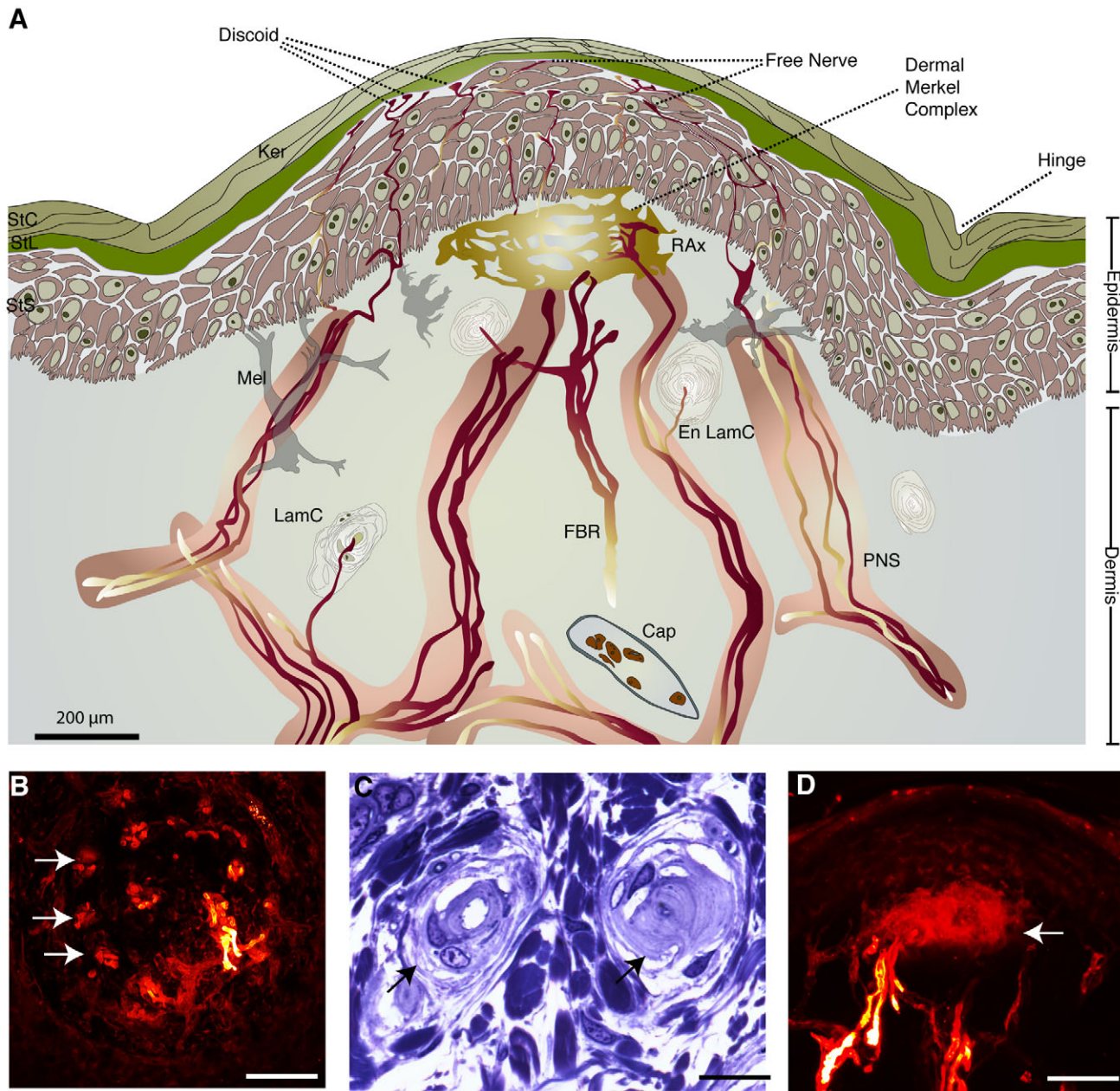


Fig. 4. The structure of the crocodilian ISO. (A) Schematic representation based on samples from *A. mississippiensis* and *C. niloticus* cranial and body receptors. A diverse array of tactile components was localized to the epidermis and dermis of the ISO. Discoid receptors with enlarged terminals and free nerve endings ran through the keratinized epidermal layers that overlaid the prominent dermal Merkel complex and large branching network of myelinated axons. Cap, capillary; Discoid, discoid receptor; En LamC, encapsulated lamellated corpuscle; FBR, free branched receptor of the connective tissue; Ker, β -keratinocyte; LamC, lamellated corpuscle; Mel, melanocyte; PNS, perineural sheath; RAx, branched receptor axons of the ISO connective tissue; StC, stratum corneum; StL, stratum lucidum; StS, stratum spinosum. (B) Confocal fluorescence of Dil-labeled free nerve endings (arrows) from a section tangential to the surface of the receptor, 20 μ m below the apex. Scale bar, 10 μ m. (C) Lamellated corpuscles (arrows) were visible in Toluidine-Blue-stained sagittal sections from the dermis of the receptor. Scale bar, 50 μ m. (D) A large dermal Merkel complex (arrow) and related branches of Dil-labeled nerve fibers as seen under confocal microscopy in a cross-section. Scale bar, 200 μ m.

circumference of the dome when viewed in horizontal sections, with nerve endings branching from larger groupings. At lower levels, the myelinated bundles were markedly larger in diameter ($75 \pm 13 \mu$ m).

Cleared specimens stained with Sudan Black B revealed the origin of the nerves in the trigeminal system (Fig. 5). This preparation was useful for identifying the large rami of the trigeminal nerve and for following the finer terminals to areas

covered in ISOs (Fig. 5B). These data are shown in the schematic created from two hatchling alligators. A stained specimen from a juvenile Nile crocodile showed a similar pattern of innervation. The trigeminal nerve bifurcated into the mandibular and maxillary/ophthalmic lobes ~ 1 to 2 mm from the Gasserian ganglion. The mandibular nerve then ran through the external mandibular fenestra and extended both caudally to the back of the angular bone and rostrally to the teeth and anterior portions

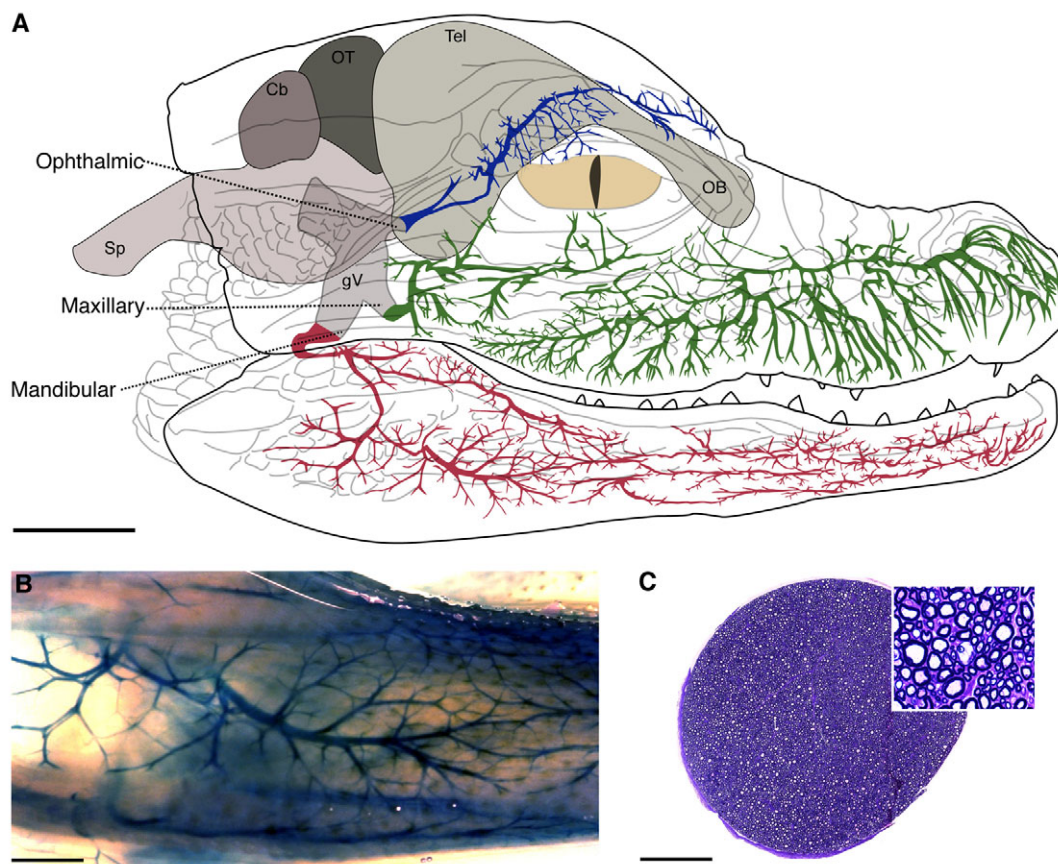


Fig. 5. Innervation of the cranial ISOs by the trigeminal nerve. (A) Side view of the rami of the trigeminal nerve with hypertrophied mandibular and maxillary branches comprising a network of finer fibers innervating regions where ISOs are present. Branching patterns were drawn from Sudan Black B preparations (see Materials and methods). The brain is shown to indicate the relative location of the trigeminal ganglion. Cb, cerebellum; gV, trigeminal ganglion; OB, olfactory bulb; OT, optic tectum; Sp, spinal cord; Tel, telencephalon. Scale bar, 1 cm. (B) Example photograph of Sudan Black B preparation showing the darkly stained processes of the maxillary nerve within the cleared whole-mounted specimen. Scale bar, 750 μ m. (C) Transverse section of a mandibular nerve from *C. niloticus*. More than 46,000 myelinated axons (s.d.=2700), as seen in the inset, were present within the nerve whereas fewer (3600 \pm 200) were present in the ophthalmic component. Scale bar, 50 μ m.

of the dentary. From the fenestra, the mandibular ramus branched extensively into at least three smaller ramules running parallel to the mandible and narrowed as it extended rostrally. The maxillary ramus ran from the jugal and quadratojugal and appeared equally diverse in its arborization near the ISOs. Both the dentary and the maxilla had many small foramina, and nerve fibers ran through the bone to project out of these openings in both directions on the rostrocaudal axis. Typically, the afferents of a single cranial foramen innervated three ISOs. In addition to supplying fibers to the external surface of the jaws, both the mandibular and maxillary rami innervated the palate and gingivae extensively, both of which were covered in ISOs.

The ophthalmic ramus, which mainly innervated the largely receptor-free nasal and lacrimal bone areas as well as the dorsomedial surface of the cranium, was much smaller than the mandibular and maxillary rami and did not branch extensively. In four yearling alligators, the mandibular and maxillary rami contained $\sim 46,500 \pm 2700$ and $48,300 \pm 3300$ myelinated axons, respectively, whereas the ophthalmic ramus contained only 3600 ± 200 myelinated fibers. Similarly, in four Nile crocodiles matched in age and body size to the alligators, there were $\sim 46,300 \pm 2800$ myelinated axons in the mandibular, $49,400 \pm 3000$ in the maxillary and 3300 ± 300 in the ophthalmic rami.

Responses of neurons in the trigeminal ganglion

The trigeminal ganglion was found ventral to the ear, behind the jugal in anatomical dissections. To examine the responses of the cranial ISOs, we recorded extracellular activity from afferent cell bodies in the ganglion. We began by characterizing the location and size of receptive fields corresponding to multi-unit activity elicited by stimulating the skin with fine wooden probes and calibrated von Frey hairs. Receptive fields were found for the majority of the skin surfaces across the face of each crocodilian, including areas on the external surface of the mandible, the maxilla, the jugal bones ventral to the eye, and within the oral cavity, among other regions. The extent of these multi-unit fields was documented and then single units were isolated to investigate individual afferents in greater detail.

The majority of receptive fields corresponded to skin areas covered in ISOs (Fig. 6). Large receptive fields were found across the jaws and often extended ventrally across the mandible or dorsally to areas near the nares on the maxilla. Although some receptive fields were located on facial areas where ISOs were absent (i.e. the skin area dorsal to the suprangular and ventral to the quadratojugal), the majority of responses were elicited by stimulation on or near ISO-covered skin. Furthermore, receptive fields were organized in an overlapping manner, with the same area of ISOs often represented in two different locations in the ganglion. Ganglion cells responsive

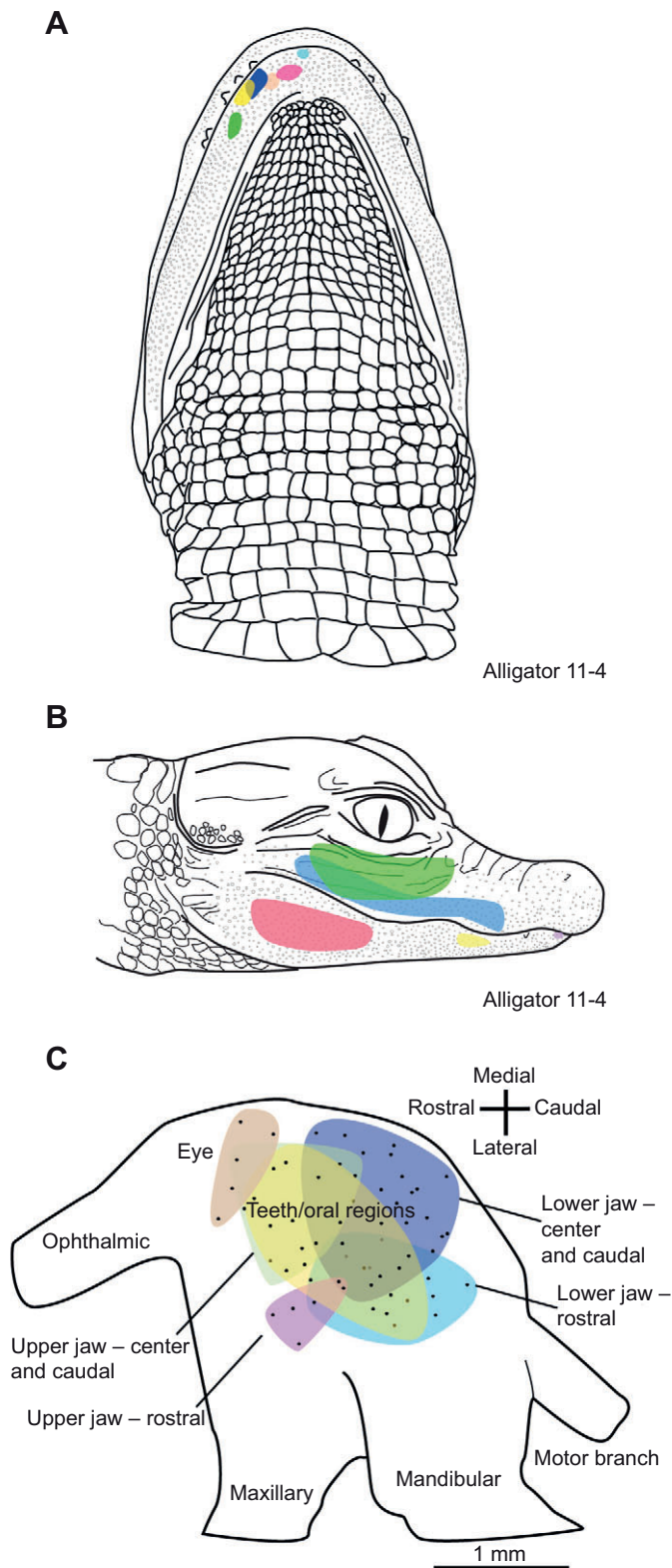


Fig. 6. Representations in the trigeminal ganglion. (A) Ventral view of the lower jaw with representative receptive fields, which were often small and near the rostral margins of the head. (B) Side view from the same case, showing the larger, overlapping fields that are characteristic of the more caudal regions of the dentary and maxilla. (C) Composite figure from 10 *A. mississippiensis* and two *C. niloticus* trigeminal recording cases. Large regions representing the teeth and mouth are present on the center of the body of the trigeminal ganglion, while a smaller region located rostrally contains neurons responding to the ISO-sparse areas near the eye.

to mechanical stimulation near the eye were located rostromedially near the ophthalmic branch whereas cells responsive to mechanical stimulation of the upper and lower jaws were found more caudally in the ganglion. A large area of the ganglion between the maxillary and mandibular branches contained cells that responded to stimulation of the teeth, upper palate and tongue (Fig. 6C).

In total, 216 single units from the trigeminal ganglion were recorded and analyzed in juvenile alligators, and 53 were examined in Nile crocodiles. Their receptive fields were plotted on photographs taken of each individual crocodilian. In general, the tactile receptive fields corresponding to the most rostral regions of the animal's face were smallest and more numerous compared with those corresponding to caudal regions innervated by the mandibular and maxillary nerves (Fig. 6A,B). The smallest receptive fields encompassed single ISOs, with surface areas of less than 1 mm^2 . These fields comprised of a single ISO were most often (92%) found near the rostral aspect of jaws, though a few were found on more caudal regions of the face. Larger cranial receptive fields contained more than 240 ISOs and were as much as 130 mm^2 in area (not illustrated).

After recording the area of each receptive field, mechanosensory thresholds were measured using calibrated von Frey hairs. We found that wet skin surfaces provided lower thresholds compared with dry skin, and thus all recorded data came from preparations with moisture maintained. Among the 174 single unit receptive fields measured for indentation force, results ranged from 13.725 to 0.078 mN, corresponding to von Frey filaments numbered 4.17 to 1.65, respectively. The lowest threshold could not be established for the 28 receptive fields that were sensitive to the 1.65 filament as this was the smallest calibrated force that could be applied. The most sensitive areas were concentrated near the rostral premaxilla and mandible, as well as in apposition to the teeth. All of the receptive fields that were restricted to a single ISO were responsive to the 0.078 mN (smallest) indentation force. Afferents with the highest thresholds were generally found near the relatively sparsely innervated regions on the dorsal surface of the maxillary, between the nares and the eyes, and at the caudal margins the jaws. In general, afferents that were activated by the least pressure had small receptive fields whereas afferents responding to the stimulation of many ISOs (large receptive fields) required greater force (13.725 mN or more).

To investigate the responses of afferents to precisely controlled stimuli, we employed a dedicated mechanosensory stimulator (Chubbuck, 1966). The Chubbuck stimulator was driven by a sine wave or square wave generator that controlled the linear movement of a small probe in a single dimension. The probe's location was precisely tracked by a calibrated analog output of the stimulator (Fig. 7).

Afferents that responded to the onset and offset of square-wave stimuli were characterized as rapidly adapting (RA) (Fig. 7E,D, Fig. 8) whereas afferents that responded throughout the duration of the stimulus were characterized as slowly adapting (SA) (Fig. 7A,D,F). The SA responses could be further subdivided into SA I and SA II, based on the coefficient of variation (CV) of the interspike interval (ISI) during the static phase (200 to 500 ms) of the maintained stimulus. This was calculated as the standard deviation of the ISI divided by the mean ISI for the 2 s train of action potentials (Chambers et al., 1972; Wellnitz et al., 2010). SA I units displayed irregularly timed discharges in response to the maintained stimulus whereas SA II units had regularly timed discharges during the same period. Among 110 units in four alligators, 51% of the responses were RA and 49% were SA

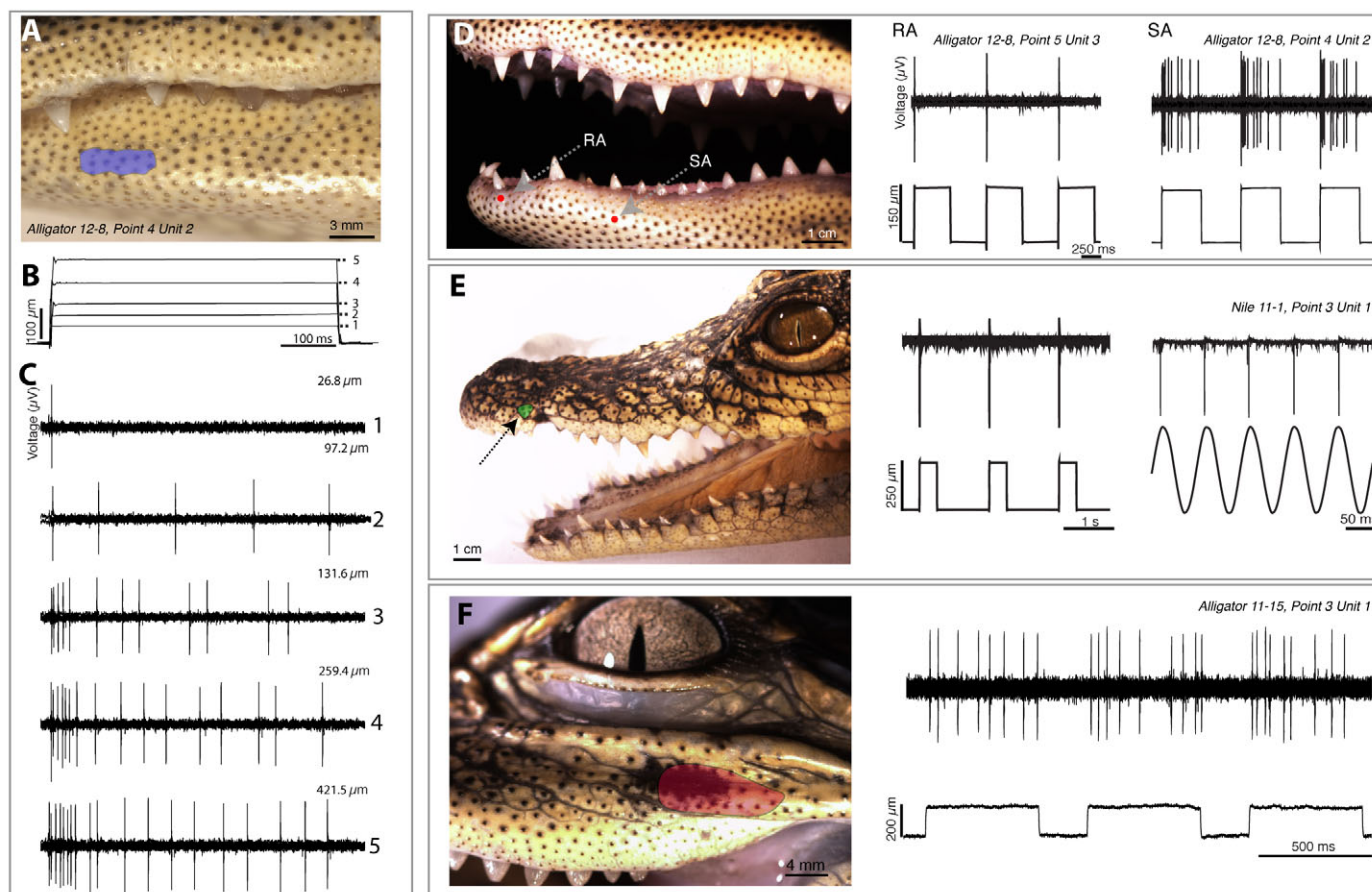


Fig. 7. Responses of trigeminal afferents from ISO-covered skin in crocodilians. (A) The small receptive field located on the juvenile *A. mississippiensis*. (B) Recording of the movement of the stimulator based on a calibrated analog output proportional to displacement. (C) Response of the afferent to the displacements shown in B showing the discharge pattern of a typical slowly adapting (SA) type II afferent. The interspike interval increased monotonically with increased displacement amplitude, maintaining the 'regular' firing pattern indicative of SA type II fibers. In D–F, the output of the stimulator is recorded below the response of the afferent. (D) SA (in this case type I) and rapidly adapting (RA) responses were present for receptive fields covering individual ISOs near the teeth in this *A. mississippiensis* case. (E) An RA unit from a juvenile *C. niloticus* is shown responding to block and sinusoidal (20 Hz) stimuli. The photograph of the crocodile has been reversed to show the small receptive field more clearly. (F) Larger receptive fields, covering multiple ISOs, were found at the caudal margins of the jaws as illustrated in an *A. mississippiensis* case.

(Table 1). Of the slowly adapting responses, 39% were SA I and 37% were SA II. The remaining 24% of the SA responses had CVs that were more than the 0.30 cut-off for SA II but less than the 0.50 cut-off for SA I responses. The Chubbuck stimulator was not used on a comparable number of Nile crocodile afferents, but based on classification of 15 afferents from two Nile crocodiles using handheld probes, similar proportions of RA and SA units were found (55% SA and 45% RA responses).

Among a set of RA responses ($N=14$), neurons were maximally phase-locked with one-to-one correspondence of response per stimuli cycle to the lower vibrations (10 to 35 Hz) and were less attuned to 100 Hz, 200 Hz, 300 Hz, and higher-frequency stimuli (Fig. 8). Furthermore, smaller displacements of the probe were required to elicit responses for 20–30 Hz vibrations compared with lower- (5 and 10 Hz) or higher-frequency (50, 75, 100, 150 and 200 Hz) stimuli. RA units continued to respond to frequencies greater than 350 Hz in four cases, and the median highest frequency for the SA responses was 250 Hz in the SA II units.

In order to test for other possible sensory functions of the cranial ISOs, we monitored activity in response to hyperosmotic solutions and to electric fields ($N=40$ afferents in four alligators and $N=15$

afferents in two crocodiles). Single-unit neuronal responses were isolated as described above, and cranial regions were exposed to room-temperature deionized water and 31 to 47 p.p.t. sea salt solutions. These were applied *via* pipette or swab to the specific receptive field and allowed to remain for at least 3 min. No single- or multi-unit activity was detected apart from responses to the force of the initial application of the solution. In other cases, the head of the crocodilian was lowered into a tank of room-temperature water, immersing the previously identified receptive field while the electrode was held in place. A 9 V battery was placed in the water and moved in different configurations around the head, similar to paradigms used to elicit electrolocating behaviors in platypus (Scheich et al., 1986). No single- or multi-unit responses were observed.

Responses of the spinal nerves

The forelimb of the crocodile was supplied by the median, radial and ulnar nerves, and all three ran to the five digits as well as to the skin of the dorsal surface of the limb (Fig. 9A). The three nerves were exposed near the proximal humerus. An electrode was inserted into the nerve, and single unit responses were recorded. In total, 67

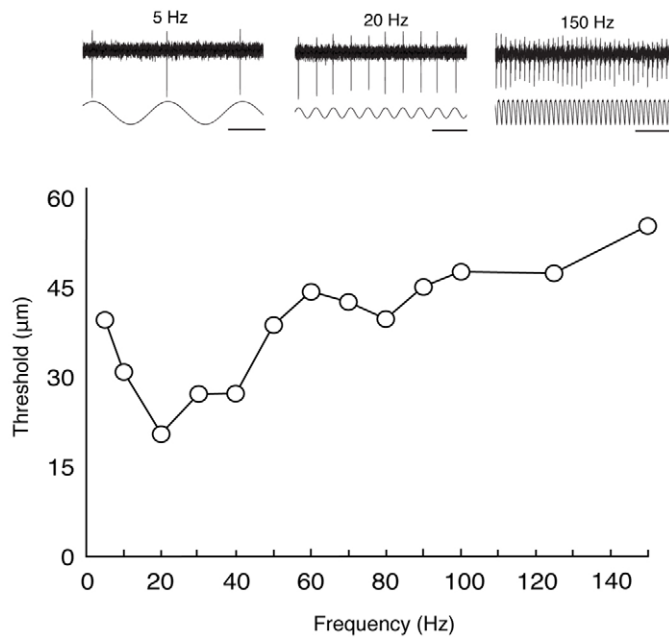


Fig. 8. Tuning curve for an *A. mississippiensis* cranial ISO. Upper panels: recordings of 1:1 entrained responses from one trigeminal *A. mississippiensis* RA unit to sinusoidal stimulation of increasing frequency. The movement of the stimulator is illustrated below each afferent recording. Scale bars, 100 ms. Lower panel: the threshold displacement of the probe required to produce 1:1 entrained responses for a single afferent from 10 to 150 Hz. Thresholds were lowest in the 20–30 Hz range and were greater with both lower and higher frequencies. Tick marks on the x-axis indicate 10 Hz intervals.

single units from two alligators and 45 units from two crocodiles were examined from the medial, radial and ulnar nerves. For both body regions, receptive fields were drawn on the photographs of the animal.

The receptive fields found on the limbs of the alligators ranged from less than 1 mm² to more than 58 mm² (mean \pm s.d. = 16.4 \pm 11.5), and the largest were found on the anterior surface of the hindlimb, above the tibia. On the forelimb, the smallest examples were isolated

to the distal regions of the digits of the forelimb. In particular, digits IV and V had minute receptive fields near the 'fingertip' areas. These digits are notable in that they lack the claws found on digits I to III, were more slender, and appeared to be proportionally reduced in crocodilians compared with other reptile groups (Vargas et al., 2008). They have also been speculated to have a specialized tactile role in detecting tactile stimuli from aquatic prey (Vliet and Groves, 2010). Numerous low threshold receptive fields were found distributed on the distal portion of these digits as well, with afferents responding to indentation forces of 0.392 mN or less. There was an orderly progression of sensitivity as one moved more proximally up the limb with the dorsal surface of most digits responding to the forces between 0.686 and 1.569 mN, to regions covering the carpals responding to 0.392 to 9.804 mN, then to areas covering the radius and ulna responding to forces of 13.725 mN (Fig. 9B,C). Other areas of heightened sensitivity included the webbing between digits I through III.

The hindlimb followed a similar pattern such that afferents from distal portions of the digits had small receptive fields and responded at the lowest thresholds, whereas afferents innervating areas over the tibia and fibula had larger receptive fields and responded at higher thresholds. By exposing the median and saphenous nerves near the proximal end of the femur, recordings were obtained for much of the hindlimb and its plantar surface (Fig. 10). In recordings from the forelimbs and hindlimbs in both species of crocodilians, both RA ($N=18$ in Nile crocodiles; $N=29$ in alligators) and SA afferents ($N=27$ in Nile crocodiles; $N=39$ in alligators) were observed.

In all of the electrophysiological recordings, the relationship between receptive field surface area and the threshold force necessary to elicit activity was noted. In both alligators and Nile crocodiles, smaller receptive fields were correlated with lower displacement forces on the face (alligators: Spearman's $\rho=0.651$, $N=127$, $P<0.001$; crocodiles: Spearman's $\rho=0.5664$, $N=16$, $P=0.0222$) and body (alligators: Spearman's $\rho=0.618$, $N=67$, $P<0.001$; crocodiles: Spearman's $\rho=0.6506$; $n=45$, $P<0.001$). Likewise, larger receptive fields were correlated with greater displacement forces.

We also tested for responses to salinity changes or electric fields. The receptive field of interest on the limb was identified and

Table 1. Response properties of afferents of the ISO-covered scales from the trigeminal ganglia of four juvenile *Alligator mississippiensis*

Type	Number	%	RF area (mm ²)	Mean area (mm ²)	Median min. displacement (μm)	Median threshold (mN)	Highest frequency response (Hz)	Associated structures	Discharge pattern	Coefficient of variation
RA	56	50.9	0.07–45.51	6.34 \pm 1.23	24.18	0.08	350	Lamellated corpuscles	At onset and offset only	–
SA I	21	19.1	0.18–15.46	6.48 \pm 0.24	52.58	0.08	250	Merkel discs and cells	Irregular discharges to maintained stimulus	<0.30
SA II	20	18.2	0.03–20.12	4.81 \pm 0.30	41.53	0.3	200	Specialized end organs	Regular discharges to maintained stimulus	>0.50
SA indeterminate	13	11.8	0.08–5.78	2.45 \pm 0.61	22.19	0.08	250	–	Regular and irregular discharges to maintained stimulus	0.30–0.50
Total	110									

ISO, integumentary sensory organ; RA, rapidly adapting response; SA I, slowly adapting type I response; SA II slowly adapting type II response.

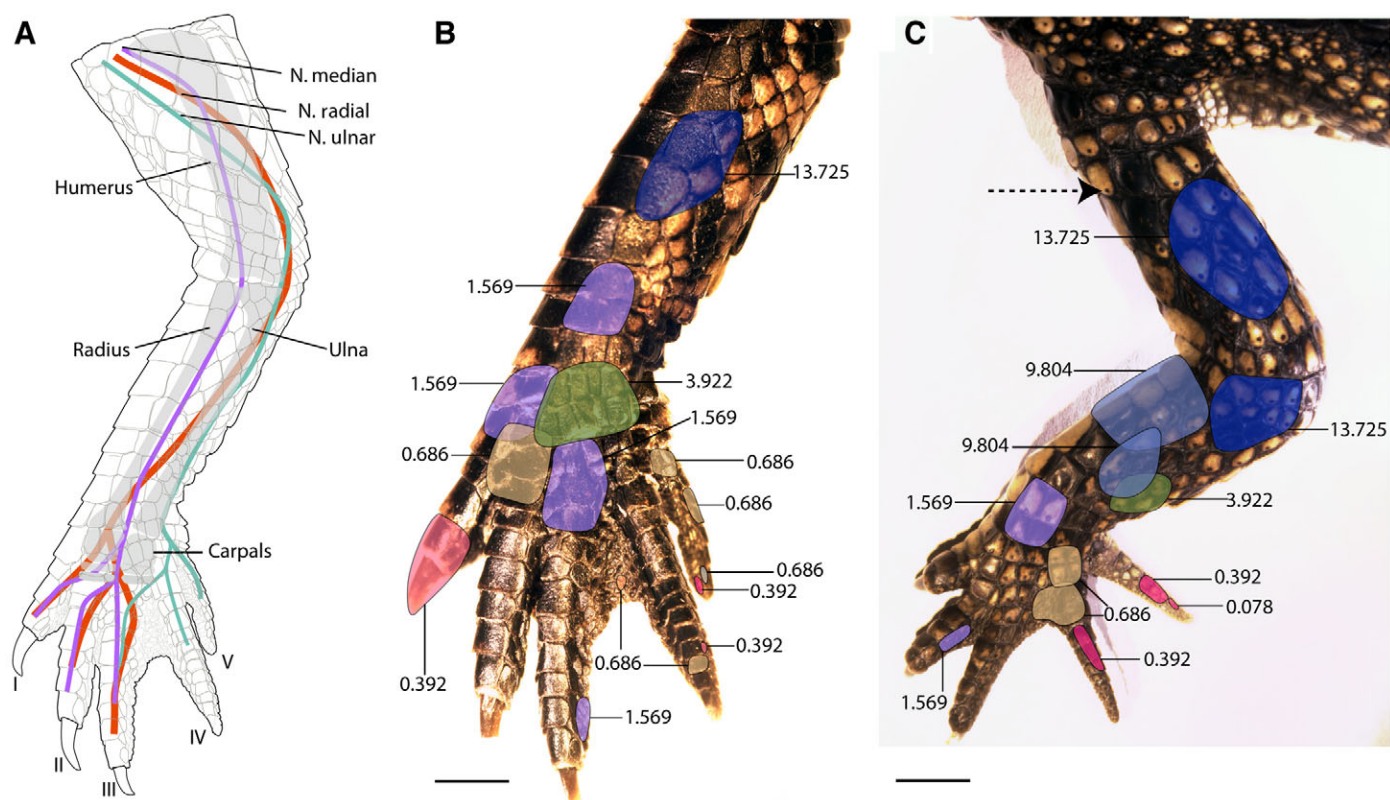


Fig. 9. Receptive fields of the forelimb in crocodilians. (A) In order to record from the forelimb, individual single units were isolated in the median, radial and ulnar nerves near the proximal areas of the humerus. (B) Select receptive fields of single peripheral afferents from an *A. mississippiensis* case. The numbers represent the indentation threshold from the von Frey filament, measured in mN. Scale bar, 1 cm. (C) Select receptive fields in a *C. niloticus* case. Individual body ISOs are visible as small black dots on each scale (black dotted arrow). Same conventions as in B.

examined for threshold sensitivity and then the animal was positioned to allow the body region to be submerged in a container filled with distilled water or 31 to 47 p.p.t. sea salt solution (Fig. 10). Immersing the limb in room-temperature water or hyperosmotic sea salt solution, as monitored for at least 3 min, evoked no observable single- or multi-unit responses in either alligators or crocodiles. Similarly, there were no responses to the 9 V battery in the water.

Behavior

Juvenile crocodilians, ranging in age from hatchling (SVL=10.2 cm) to 3 years (SVL=76.2 cm) were observed and videotaped orienting towards and capturing prey or ingesting food pellets dropped into the water. With full-spectrum lighting, they generally turned rapidly towards water ripples generated by dried food pellets dropped from above. Often, they closed both their lower, movable nictitating membrane and external eyelids as they snapped laterally towards the initial source of the disturbance. Although the jaws often secured the food with the initial bite, subsequent bites re-orienting toward the item appeared to rely on direct contact with the submerged pellet because the closed eyes were positioned well above the water surface (supplementary material Movie 1, clip 1). These sideways snaps of the jaws were directed toward the food pellet within 50 to 70 ms of the item's contact with the skin.

Crocodilians were also monitored under 940 nm IR illumination and with white noise to block auditory cues. Both alligators and crocodiles were capable of orienting towards the location of water disturbances when floating with their heads at the water surface. When positioned in this manner, the areas of greatest ISO density

near the rostral margins of the jaws and adjacent to the teeth were often below the air–water interface and just the eyes, ear flap and more dorsal regions of the maxilla were exposed. Following the initial directed movement towards the water disturbance (supplementary material Movie 1, clip 2), both alligators and crocodiles often swept their heads laterally when in the area of the source of the ripples (Fig. 11, supplementary material Movie 1, clips 3 and 4). The animal was obviously searching for the source of the disturbance and often continued for 3–4 s or until its jaws touched an object. Within 200 ms of contact with the object, the crocodilian usually bit the item and began to attempt ingestion. In the event that the animal had inadvertently secured a non-edible item (such as floating aquarium fauna), the object was released after several snaps of the jaws whereas edible objects were quickly eaten.

Crocodilians were also observed orienting towards freely swimming fish under IR illumination. Despite facing the opposite direction and having their heads above water, crocodiles were capable of rapidly turning and diving underwater towards the location of the fish (supplementary material Movie 1, clip 5). In another predatory strategy, crocodiles would often remain submerged until prey came into contact with the skin surfaces (supplementary material Movie 1, clip 6) or the open mouth (supplementary material Movie 1, clip 7), at which point the animal immediately attempted to capture the fish in its jaws.

DISCUSSION

Alligatorids have a dense array of sensory receptors (ISOs) extending around the mouth and cranial regions (4200 ± 94 ISOs in *A.*

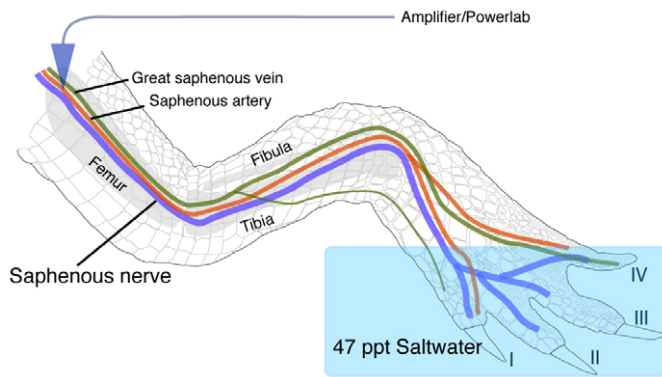


Fig. 10. Electrophysiological recording preparation as used in body recordings. In this case, the single-unit responses from the hindlimb were recorded from the saphenous nerve. Once units were identified mechanically, the receptive field was submerged in hyperosmotic solutions to monitor for activity. No activity related to immersion in the saltwater solution was detected.

mississippiensis) whereas crocodylids have ISOs distributed across almost every scale of the body surface (6200 ± 389 ISOs) as well as on the head (2900 ± 134 ISOs in *C. niloticus*). Since the earliest reports of ISOs (Maurer, 1895; von Wettstein, 1937) and their use in the dichotomous identification of crocodilian skins (King and Brazaitis, 1971), their function has remained a topic of speculation. Although detailed morphological studies undertaken in *Caiman* receptors (von Düring, 1973; von Düring, 1974; von Düring and Miller, 1979) strongly suggested a mechanosensory role for ISOs, physiological characterization of their function has been limited to the trigeminal receptors of a single species (*A. mississippiensis*) (Soares, 2002). Anatomical studies of crocodylid post-cranial ISOs from *Crocodylus porosus* focused on a potential role of the organs as osmoreceptors (Jackson and Brooks, 2007; Jackson et al., 1996). This hypothesis is based in part on models of how ISOs mechanically flatten under osmotic pressure in a saltwater environment and on experiments measuring the mass of water consumed by the estuarine crocodiles. This led to the hypothesis that ISOs are the first identified vertebrate integumentary osmoreceptors (Jackson and Brooks, 2007). Other investigators have proposed that ISOs could function as magnetoreceptors (Rodda, 1984) or electroreceptors (Bullock, 1999).

Structure of ISOs

The ISOs appear to share many structural similarities with known mechanoreceptors. These include the push-rod receptor organs distributed across the snouts of monotremes (Andres and von Düring, 1984; Andres et al., 1991) and the Eimer's organs found on the glabrous skin on the rhinarium of moles (Catania, 1995). Numerous 'Tastflecken' ('touch spots') found on the small warts of bufonid toads and ranid species of frogs have also been identified (Lindblom, 1963; Ogawa et al., 1981). Cutaneous cephalic corpuscles with protruding centers appear in some colubrid snakes (Jackson, 1971; Jackson and Doetsch, 1977). Herbst and Grandry corpuscles comprise the tactile bill tip organs found in ducks (Berkhoudt, 1979; Gottschaldt and Lausmann, 1974). In all these cases, the receptor appears as a smooth, domed structure with an apex suitable for transducing deflection to a series of specialized afferents.

In juvenile crocodilian ISOs, the external, keratinized dome typically had a diameter of 0.5 mm or less for those distributed across

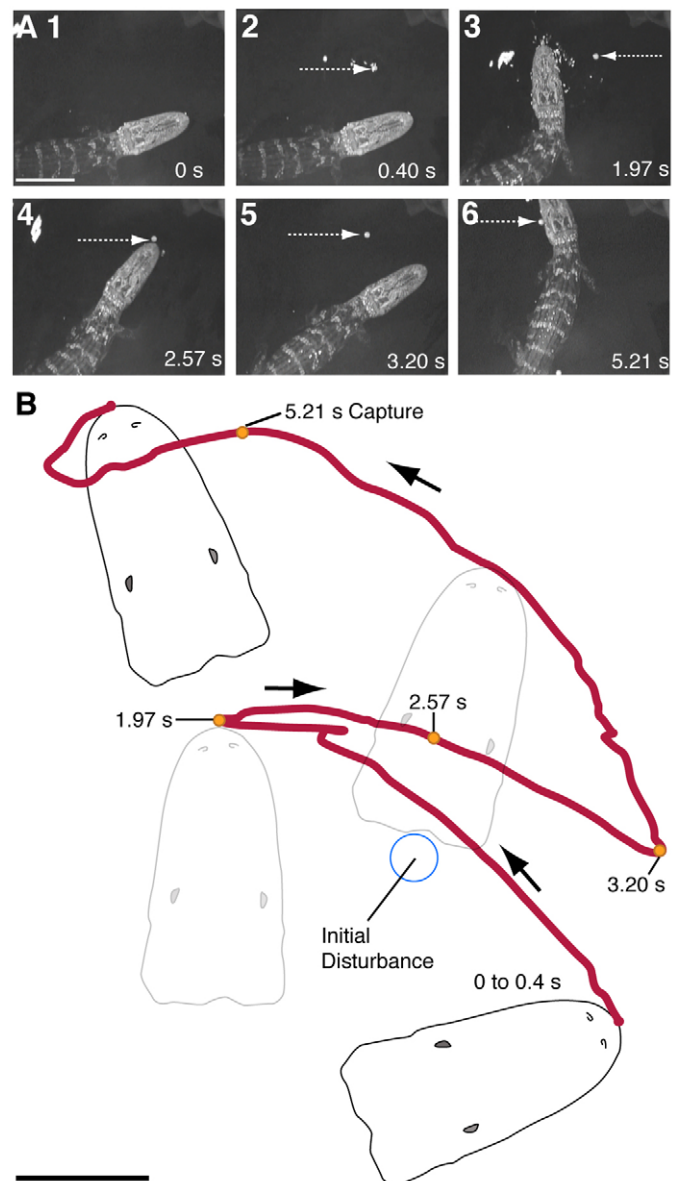


Fig. 11. Crocodilian behavioral responses following water surface disturbance. (A) Individual images from a film sequence recorded under infrared lighting and white noise presentation to block audition as a juvenile *A. mississippiensis* orients towards a surface wave generated by a small food pellet (white arrows). (B) Schematic of the orienting movements presented in A. From the animal's initial location, a lateral, sweeping head movement is repeated until the head makes tactile contact with the floating pellet and it is rapidly captured. Scale bar, 10 cm.

the jaws whereas larger ISOs (1.2 mm) were found on crocodylid body scales. Despite this size difference, both populations of ISOs appeared remarkably similar in internal composition. The stratum corneum is thin over the organ (5 μ m), presumably allowing a range of motions to compress the structure. This layer of three to five β -keratin cells (Alibardi, 2011) functions both in structural integrity of the ISO and acts as scaffolding for the most apical of the fine nerve terminals. In transverse sections, highly branched melanocytes can be seen throughout the keratinized layers and underlying collagenous layers and impart the distinctive pigmentation seen in most of the ISO bodies. A number of mechanoreceptors are apparent

in sectioned ISOs. These mechanoreceptors can be broadly categorized based on their morphology and distribution, as described by von Düring and Miller (von Düring and Miller, 1979). These distinctions are as follows: (1) receptors of the epidermis, (2) receptors of the connective tissue with Schwann cell elaborations or myelination, (3) receptors of the connective tissue lacking Schwann cells and (4) Merkel cell neurite complexes. Among tactile specializations of the first group, crocodilians, as well as reptiles more generally (Landmann and Villiger, 1975; von Düring, 1973), are notable for having expansions of the receptor terminals, compared with the finer, tapered free nerve terminals found in most other vertebrates (Fig. 4B). The dermal Merkel column, similar to the ubiquitous epidermal Merkel neurite complex, traditionally has been interpreted as slowly adapting in other species. These columns were isolated to regions under each ISO whereas similar Merkel cells are found ubiquitously across the epidermal body surface in fishes (Lane and Whitear, 1977), amphibians (Nafstad and Baker, 1973), birds (Nafstad, 1971) and mammals (Halata, 1970; Munger, 1965). Lamellated corpuscles, comparable to the paciniform structures of mammals (Pease and Quilliam, 1957), have been characterized as rapidly adapting (Andres and von Düring, 1973; Iggo and Muir, 1969; von Düring and Miller, 1979). Indeed, both rapidly adapting and slowly adapting afferents were observed in our physiological data.

The close association between the discoid terminals and the supporting epidermal cells of the stratum corneum and lucidum has been observed before in reptile scales (von Düring and Miller, 1979) and in mammalian glabrous skin (Munger and Ide, 1988), and this relationship also holds for the crocodilian ISOs both from the cephalic and body regions. Highlighting the intimate association with the free nerve terminals, fluorescent lipophilic label (DiI) applied to bundles of myelinated fibers of the maxillary nerve often labeled the keratinized epidermal layers directly over the ISO while remaining absent from adjacent scaled regions.

Several features of the trigeminal system of crocodilians stood out when examining the innervation of the cranium. First, there was an exceptional density of nerve fibers supplying the skin of the face and a vast network of branching nerve bundles just below the epidermis. Throughout the dermis, ensheathed groups of myelinated afferents projected across the rostro-caudal length and outwards towards the epidermis, as seen in the cleared Sudan Black B specimens. The bundles emerged through small foramina of the maxilla and dentary. This organization is reminiscent of mechanosensory end organs found in the foramina of anterior margins of the beaks of water-foraging birds with bill tip organs (Cunningham et al., 2010) and highlights the shared archosaurian phylogeny between crocodilians and birds (Hedges and Poling, 1999). It seems likely that by having the majority of the maxillary and mandibular nerves shielded in bone, crocodilians are armored against many potential injuries that might be encountered when feeding communally, while simultaneously maintaining an acutely sensitive skin surface *via* the fibers running through the foramina.

Trigeminal afferents and their organization

A large proportion of the neurons in the trigeminal ganglion responded to stimulation of the areas most densely covered in ISOs near rostral points of the pre-maxilla and mandible and surrounding the teeth. In addition, many afferents responded to very light contact to the teeth, underscoring previous ultrastructural investigations of sensory nerve endings within the dental ligament and attachment tissues in *Caiman crocodilus* (Berkovitz and Sloan, 1979; Tadokoro et al., 1998). In general, the smallest receptive fields were found

rostrally on the upper and lower jaws and near the teeth. This overall pattern of small receptive field size and corresponding 'overrepresentation' in the ganglion is reminiscent of cortical magnification of behaviorally important skin surfaces observed in mammals (Krubitzer, 2007; Sur et al., 1980). For many species, the most important skin surfaces used for exploring objects are densely innervated by afferents with the smallest receptive fields, and the skin surfaces have correspondingly large representations in the central nervous system. Examples of functionally significant skin surfaces with consequently large nervous system representations include the forelimb of the raccoon (Welker and Seidenstein, 1959), the bill surface in the platypus (Pettigrew, 1999) and the lips and tongue of humans (Penfield and Boldrey, 1937). The overall pattern found for crocodilians, which have the highest density of ISOs and smallest receptive fields around the teeth, provides an important clue to ISO function. We suggest that ISOs play a key role not only in capturing prey based on water movements (Soares, 2002) and contact, but also in discriminating objects that have been grasped in the jaws and guiding the manipulation of prey once it has been secured. This interpretation is consistent with other recent findings in vertebrates that have revealed very large cortical representations of the dentition and oral structures that had been previously unappreciated (Jain et al., 2001; Kaas et al., 2006; Remple et al., 2003).

Within the ganglion, neurons that responded to the rostral head were typically located ventrolaterally whereas neurons responding to stimulation of the caudal regions of the jaws were positioned dorsomedially. As would be expected, responses to stimulation of the pre-maxilla, maxilla and quadratojugal of the upper jaw were recorded from the anterior regions of the ganglion, in proximity to the entrance of the maxillary nerve into the ganglion, and areas responsive to stimulation of the dentary were recorded from the posterior regions, near the mandibular nerve's division from the ganglion. The electrophysiologically derived topography of the crocodilian trigeminal ganglion was consistent with maxillary representations in the maxillo-mandibular lobe as documented in horseradish peroxidase tracer studies from hatchling chicks (Noden, 1980).

In both the Nile crocodiles and alligators, receptive fields, some as small as the area of a single ISO, were sensitive to indentation thresholds produced by the finest von Frey filaments corresponding to a force of 0.078 mN. These measurements represent sensitivities more acute than those of primate fingertips (Johansson et al., 1980) – skin surfaces that are widely appreciated for their sensitivity (Darrian-Smith, 1984; Kaas, 2004). Similarly, tactile responses were elicited by mechanical displacements as small as 3.9 µm – an indentation threshold lower than found for the human hand (Johansson, 1978). These findings are evidence of the extreme and surprising sensitivity of the crocodilian face and may represent a requirement for the detection of subtle water disturbances (Soares, 2002) in addition to the discrimination of different objects and prey.

RA, SA I and SA II type responses were identified in recordings from the surface of single trigeminal ISOs of alligators as well, in keeping with the diverse array of mechanoreceptors and afferent end organs found in each receptor. A prior electrophysiological study from the plantar nerve of alligators and caiman, which lack ISOs on the body, have also found RA, SA I and SA II afferents on the hindlimbs (Kenton et al., 1971). However, in this preceding study, the finest indentation forces found for these cutaneous regions lacking ISOs (as is the case in alligatorid limbs) were more than six times greater than the median indentation forces for responses from the ISO covered areas (0.08 mN) in this report, suggesting that

the organs provide a considerable increase in sensitivity. ISOs therefore seem to be structures that impart great sensitivity to an otherwise armored and shielded body surface.

Analysis of 14 RA responses collected for stimulus frequencies up to 350 Hz indicated that the lowest indentation thresholds were found at 20–30 Hz within the 5–150 Hz range. Larger displacement distances were necessary to elicit 1:1 entrained responses of the afferent to frequencies both below and above the 20–30 Hz window. The 20 Hz vibration stimulus has been noted as one of the optimal frequencies to induce orientation behaviors towards water surface disturbance in *Notonecta glauca* – a predatory aquatic insect that localizes and orients towards prey-borne surface waves transmitted via mechanoreceptive tarsal scolopoidal organs and abdominal sensory hairs (Lang, 1980; Weise, 1974). Thus the tuning of afferents to this frequency in crocodilians is consistent with prior behavioral observations of juvenile alligators orienting towards water surface ripples (Soares, 2002). In addition, responses from SA (both types I and II) and RA units often extended beyond 200 and 300 Hz and were elicited by 40–80 µm displacements, suggesting that relatively higher-frequency vibrations can also be readily transduced by ISOs.

Spinal nerve afferents

As one of the goals of this project was to collect physiological data regarding sensory function of post-cranial ISOs in crocodiles, it was necessary to record from spinal nerves innervating the integumentary surface. Although still responding to forces of 13.725 mN and finer, afferents from the body were not as sensitive as those distributed across cephalic regions in either crocodiles or alligators. Discrete single units across the limbs were typically large except for those found in distal regions of certain digits (IV and V on the forelimb and IV on the hindlimb). There also appeared to be sensitive regions, responding to indentation forces of 0.392 and 0.686 mN, on the webbing present between digits III and IV on the forelimb. These results are consistent with the concept of the ISOs being discrete tactile receptor units as they are present on some of the smallest scales of the body; perhaps the increased receptor density per unit area imparts a greater degree of acuity. This idea is supported by the notion that the digits IV and V of the forelimb, which are notably more slender and do not have the claws found on the other digits, might be adapted to detecting somatosensory cues when the animal is floating in the water (Vliet and Groves, 2010). When foraging for fish, *Caiman yacare* partially open their mouths and fully extend their forelimbs, adopting a ‘cross posture’, and indeed, fish have been observed nipping at the caiman’s digits (Olmos and Sazima, 1990), suggesting that tactile information from the digits could mediate predatory behaviors.

Another motivation for physiological investigation of the integument comes from Jackson’s intriguing series of experiments into the potential osmoreceptive capabilities of post-cranial ISOs of crocodiles (Jackson and Brooks, 2007; Jackson et al., 1996). However, in recording directly from the afferents innervating ISO-covered body surfaces in Nile crocodiles, no single- or multi-unit responses attributable to exposure to hyperosmotic solutions were observed. The results were similar to those from alligators that were used as an experimental control without body ISOs. Finally, no responses were detected in response to electrical stimuli (Scheich et al., 1986), suggesting that ISOs play no role in electric field detection, and by extension, that crocodilians do not have electroreception.

We suggest that the crocodilian ISOs function as part of an elaborate mechanosensory system and are adaptive to a number of aquatic behaviors. When filmed under 940 nm IR illumination, both

crocodiles and alligators readily struck at and captured fish (supplementary material Movie 1, clip 1) and occasionally oriented towards minute water surface disturbances, similar to the results reported by Soares (Soares, 2002). Beyond providing positional cues to the source of the stimuli, the ISOs are densely distributed throughout the upper palate and areas adjacent to the teeth within the oral cavity – a location unlikely to receive and transduce the pressure from expanding surface waves. Disjunct regions of greater receptor density were observed near the eye and nares, similar to supraorbital and rhinal microvibrissae areas found in mammals relying on trigeminally mediated tactile discrimination (Brecht, 2007; Ling, 1966; Lyne, 1959). When actively foraging, crocodilians open their mouths and move so as to sweep the arrays of cranial ISOs across the surface and underwater, rapidly capturing and securing objects that make contact with their heads, and releasing any non-edible matter, indicating that it is likely that they can discriminate between multiple different materials using tactile cues alone. As a testament to these discriminatory abilities, mother crocodilians often manipulate their eggs as they begin hatching, gently cracking away the shell with their teeth (part of a feeding apparatus capable of inflicting crushing bites and dismembering large prey) and allowing the hatchlings to seek protection in her mouth (Hunt, 1987; Pooley and Gans, 1976) – a situation in which blunted tactile acuity would be maladaptive. Although the question remains as to why ISO distribution differs between the alligatorid and crocodylid species, results from recording from the spinal nerves suggest that both species tested are sensitive to low thresholds of force. Some have speculated that ISOs homologous to the post-cranial populations of crocodylids are present far deeper within the integument in alligatorids (Richardson et al., 2002). While crocodilians are certainly capable of accurately ambushing and capturing prey by relying on their acute visual systems (Herich and Kruger, 1966; Pritz, 1975) in lighted conditions, even on the darkest nights, prey still face a formidable mechanosensory system if they unexpectedly come into contact with these reptiles.

ACKNOWLEDGEMENTS

We thank Dr Ruth Elsey and the staff of the Louisiana Department of Wildlife and Fisheries at the Rockefeller Wildlife Refuge for providing alligator specimens, and the assistance of Officer Walter Cook of the Tennessee Wildlife Resources Agency. We also thank Peter Brazaitis for anatomical advice and Eva Sawyer for technical assistance. These experiments would have been impossible without the contributions of Danielle Gauthier, who assisted with crocodilian care, data collection and analysis from this project’s inception.

FUNDING

This research was supported by the National Science Foundation [grant 0844743 to K.C.C.] and by a Vanderbilt University Discovery Grant.

REFERENCES

- Alibardi, L. (2011). Histology, ultrastructure, and pigmentation in the horny scales of growing crocodilians. *Acta Zool.* **92**, 187–200.
- Andres, K. H. and von Düring, M. (1973). The morphology of cutaneous receptors. In *Handbook of Sensory Physiology*, Vol. 2 (ed. A. Iggo), pp. 1–28. Berlin: Springer-Verlag.
- Andres, K. H. and von Düring, M. (1984). The platypus bill: a structural and functional model of a pattern-like arrangement of cutaneous sensory receptors. In *Sensory Receptor Mechanisms* (ed. W. Hamann and A. Iggo), pp. 81–89. Singapore: World Scientific Publishing.
- Andres, K. H., von Düring, M., Iggo, A. and Proske, U. (1991). The anatomy and fine structure of the echidna *Tachyglossus aculeatus* snout with respect to its different trigeminal sensory receptors including the electroreceptors. *Anat. Embryol.* **184**, 371–393.
- Berkhoudt, H. (1979). The morphology and distribution of cutaneous mechanoreceptors (Herbst and Grandry corpuscles) in bill and tongue of the mallard (*Anas platyrhynchos* L.). *Neth. J. Zool.* **30**, 1–34.
- Berkovitz, B. K. B. and Sloan, P. (1979). Attachment tissues of the teeth in *Caiman sclerops* (Crocodilia). *J. Zool.* **187**, 179–194.

- Brazaitis, P.** (1987). Identification of crocodilian skins and products. In *Wildlife Management: Crocodiles and Alligators* (ed. G. J. Webb, S. C. Manolis and P. J. Whitehead), pp. 373-86. Chipping Norton, NSW: Surrey Beatty & Sons.
- Brazaitis, P. and Watanabe, M.** (2011). Crocodilian behaviour: a window to dinosaur behavior? *Hist. Biol.* **23**, 73-90.
- Brecht, M.** (2007). Barrel cortex and whisker-mediated behaviors. *Curr. Opin. Neurobiol.* **17**, 408-416.
- Brochu, C. A.** (2003). Phylogenetic approaches toward crocodylian history. *Annu. Rev. Earth Planet. Sci.* **31**, 357-397.
- Bullock, T. H.** (1999). The future of research on electroreception and electrocommunication. *J. Exp. Biol.* **202**, 1455-1458.
- Catania, K. C.** (1995). A comparison of the Eimer's organs of three North American moles: the hairy-tailed mole (*Parascalops breweri*), the star-nosed mole (*Condylura cristata*), and the eastern mole (*Scalopus aquaticus*). *J. Comp. Neurol.* **354**, 150-160.
- Chambers, M. R., Andres, K. H., von Düring, M. and Iggo, A.** (1972). The structure and function of the slowly adapting type II mechanoreceptor in hairy skin. *Q. J. Exp. Physiol. Cogn. Med. Sci.* **57**, 417-445.
- Chubbuck, J. G.** (1966). Small motion biological stimulator. *Appl. Phys. Lab. Tech. Digest* **5**, 18-23.
- Cunningham, S. J., Castro, I., Jensen, T. and Potter, M. A.** (2010). Remote touch prey-detection by Madagascar crested ibises *Lophotis cristata urschi*. *J. Avian Biol.* **41**, 350-353.
- Darrian-Smith, I.** (1984). The sense of touch: performance and peripheral neural processes. In *Handbook of Physiology, The Nervous System III* (ed. I. Darrian-Smith), pp. 739-788. Bethesda, MD: American Physiological Society.
- Erickson, G. M., Gignac, P. M., Steppan, S. J., Lappin, A. K., Vliet, K. A., Bruegggen, J. D., Inouye, B. D., Kledzik, D. and Webb, G. J.** (2012). Insights into the ecology and evolutionary success of crocodilians revealed through bite-force and tooth-pressure experimentation. *PLoS ONE* **7**, e31781.
- Gottschaldt, K. M. and Lausmann, S.** (1974). The peripheral morphological basis of tactile sensibility in the beak of geese. *Cell Tissue Res.* **153**, 477-496.
- Grigg, G. C. and Gans, C.** (1993). Morphology and physiology of the Crocodilia. In *Fauna of Australia*, Vol. 2A (ed. C. J. Glasby, G. J. B. Ross and P. L. Beesley), pp. 326-336. Canberra, Australia: Australian Government Publishing Service.
- Halata, Z.** (1970). Nerve endings (Merkel's corpuscles) in hairless skin of the nose of the cat. *Z. Zellforsch. Mikrosk. Anat.* **106**, 51-60.
- Hedges, S. B. and Polling, L. L.** (1999). A molecular phylogeny of reptiles. *Science* **283**, 998-1001.
- Heric, T. M. and Kruger, L.** (1966). The electrical response evoked in the reptilian optic tectum by afferent stimulation. *Brain Res.* **1**, 187-199.
- Hunt, R. H.** (1987). Nest excavation and neonate transport in wild *Alligator mississippiensis*. *J. Herpetol.* **21**, 348-350.
- Iggo, A. and Muir, A. R.** (1969). The structure and function of a slowly adapting touch corpuscle in hairy skin. *J. Physiol.* **200**, 763-796.
- Jackson, K. and Brooks, D. R.** (2007). Do crocodiles co-opt their sense of "touch" to "taste"? A possible new type of vertebrate sensory organ. *Amphib.-reptil.* **28**, 277-285.
- Jackson, K., Butler, D. G. and Youson, J. H.** (1996). Morphology and ultrastructure of possible integumentary sense organs in the estuarine crocodile *Crocodylus porosus*. *J. Morphol.* **229**, 315-324.
- Jackson, M. K.** (1971). Cutaneous sense organs on the heads of some small ground snakes in the genera *Leptotyphlops*, *Tantilla*, *Sonora*, and *Virginia* (Reptilia: Serpentes). *Am. Zool.* **11**, 707-708.
- Jackson, M. K. and Doetsch, G. S.** (1977). Functional properties of nerve fibers innervating cutaneous corpuscles within cephalic skin of the Texas rat snake. *Exp. Neurol.* **56**, 63-77.
- Jain, N., Qi, H. X., Catania, K. C. and Kaas, J. H.** (2001). Anatomic correlates of the face and oral cavity representations in the somatosensory cortical area 3b of monkeys. *J. Comp. Neurol.* **429**, 455-468.
- Johansson, R. S.** (1978). Tactile sensibility in the human hand: receptive field characteristics of mechanoreceptive units in the glabrous skin area. *J. Physiol.* **281**, 101-125.
- Johansson, R. S., Vallbo, A. B. and Westling, G.** (1980). Thresholds of mechanosensory afferents in the human hand as measured with von Frey hairs. *Brain Res.* **184**, 343-351.
- Kaas, J. H.** (2004). Somatosensory system. In *The Human Nervous System* (ed. G. Paxinos and J. K. Mai), pp. 1059-1092. San Diego, CA: Elsevier Academic Press.
- Kaas, J. H., Qi, H. X. and Iyengar, S.** (2006). Cortical network for representing the teeth and tongue in primates. *Anat. Rec. A* **288**, 182-190.
- Kenton, B., Kruger, L. and Woo, M.** (1971). Two classes of slowly adapting mechanoreceptor fibres in reptile cutaneous nerve. *J. Physiol.* **212**, 21-44.
- King, W. F. and Brazaitis, P.** (1971). *Species Identification of Commercial Crocodilian Skins*. New York: New York Zoological Society.
- Krubitzer, L.** (2007). The magnificent compromise: cortical field evolution in mammals. *Neuron* **56**, 201-208.
- Landmann, L. and Villiger, W.** (1975). Glycogen in epidermal nerve terminals of *Lacerta sicula* (Squamata: Reptilia). *Experientia* **31**, 967-968.
- Lane, E. B. and Whitear, M.** (1977). On the occurrence of Merkel cells in the epidermis of teleost fishes. *Cell Tissue Res.* **182**, 235-246.
- Lang, H. H.** (1980). Surface wave sensitivity of the back swimmer *Notonecta glauca*. *Naturwissenschaften* **67**, 204-205.
- Lindblom, U.** (1963). Phasic and static excitability of touch receptors in toad skin. *Acta Physiol. Scand.* **59**, 410-423.
- Ling, J. K.** (1966). The skin and hair of the southern elephant seal, *Mirounga leonina* (Linn.) I. The facial vibrissae. *Aust. J. Zool.* **14**, 855-866.
- Lyne, A. G.** (1959). The systematic and adaptive significance of the vibrissae in the marsupalia. *Proc. Zool. Soc. Lond.* **133**, 79-133.
- Maurer, F.** (1895). *Die epidermis und ihre Abkömmlinge*. Leipzig: Wilhelm Engelmann.
- Munger, B. L.** (1965). The intraepidermal innervation of the snout skin of the opossum. A light and electron microscope study, with observations on the nature of Merkel's Tastzellen. *J. Cell Biol.* **26**, 79-97.
- Munger, B. L. and Ide, C.** (1988). The structure and function of cutaneous sensory receptors. *Arch. Histol. Cytol.* **51**, 1-34.
- Nafstad, P. H.** (1971). Comparative ultrastructural study on Merkel cells and dermal basal cells in poultry (*Gallus domesticus*). *Z. Zellforsch. Mikrosk. Anat.* **116**, 342-348.
- Nafstad, P. H. and Baker, R. E.** (1973). Comparative ultrastructural study of normal and grafted skin in the frog, *Rana pipiens*, with special reference to neuroepithelial connections. *Z. Zellforsch. Mikrosk. Anat.* **139**, 451-462.
- Necker, R.** (1974). Dependence of mechanoreceptor activity on skin temperature in sauroids. *J. Comp. Physiol. A* **92**, 65-73.
- Noden, D. M.** (1980). Somatotopic and functional organization of the avian trigeminal ganglion: an HRP analysis in the hatching chick. *J. Comp. Neurol.* **190**, 405-428.
- Ogawa, H., Morimoto, K. and Yamashita, Y.** (1981). Physiological characteristics of low threshold mechanoreceptor afferent units innervating frog skin. *Q. J. Exp. Physiol.* **66**, 105-116.
- Olmos, S. and Sazima, I.** (1990). A fishing tactic in the floating Paraguayan caiman: the cross-posture. *Copeia* **1990**, 875-877.
- Pease, D. C. and Quilliam, T. A.** (1957). Electron microscopy of the pacinian corpuscle. *J. Biophys. Biochem. Cytol.* **3**, 331-342.
- Penfield, W. and Boldrey, E.** (1937). Somatic motor and sensory representation in the cerebral cortex of man as studied by electrical stimulation. *Brain* **60**, 389-443.
- Pettigrew, J. D.** (1999). Electroreception in monotremes. *J. Exp. Biol.* **202**, 1447-1454.
- Piras, P., Colangelo, P., Adams, D. C., Buscalioni, A., Cubo, J., Kotsakis, T., Meloro, C. and Raia, P.** (2010). The Gavialis-Tomistoma debate: the contribution of skull ontogenetic allometry and growth trajectories to the study of crocodylian relationships. *Evol. Dev.* **12**, 568-579.
- Pooley, A. C. and Gans, C.** (1976). The Nile crocodile. *Sci. Am.* **234**, 114-119, 122-124.
- Pritz, M. B.** (1975). Anatomical identification of a telencephalic visual area in crocodiles: ascending connections of nucleus rotundus in *Caiman crocodilus*. *J. Comp. Neurol.* **164**, 323-338.
- Remple, M. S., Henry, E. C. and Catania, K. C.** (2003). Organization of somatosensory cortex in the laboratory rat (*Rattus norvegicus*): evidence for two lateral areas joined at the representation of the teeth. *J. Comp. Neurol.* **467**, 105-118.
- Richardson, K. C., Webb, G. J. W. and Manolis, S. C.** (2002). *Crocodiles Inside Out: A Guide to the Crocodilians and Their Functional Morphology*. Chipping Norton, NSW: Surrey Beatty & Sons.
- Rodda, G. H.** (1984). The orientation and navigation of juvenile alligators: evidence of magnetic sensitivity. *J. Comp. Physiol. A* **154**, 649-658.
- Scheich, H., Langner, G., Tidemann, C., Coles, R. B. and Guppy, A.** (1986). Electroreception and electrolocation in platypus. *Nature* **319**, 401-402.
- Soares, D.** (2002). Neurology: an ancient sensory organ in crocodilians. *Nature* **417**, 241-242.
- Sur, M., Merzenich, M. M. and Kaas, J. H.** (1980). Magnification, receptive-field area, and "hypercolumn" size in areas 3b and 1 of somatosensory cortex in owl monkeys. *J. Neurophysiol.* **44**, 295-311.
- Tadokoro, O., Mishima, H., Maeda, T. and Kozawa, Y.** (1998). Innervation of the periodontal ligament in the alligatorid *Caiman crocodilus*. *Eur. J. Oral Sci.* **106** Suppl. 1, 519-523.
- Vargas, A. O., Kohlsdorf, T., Fallon, J. F., Vandenbrooks, J. and Wagner, G. P.** (2008). The evolution of HoxD-11 expression in the bird wing: insights from *Alligator mississippiensis*. *PLoS ONE* **3**, e3325.
- Vliet, K. A. and Groves, J.** (2010). *Crocodylian Biology and Captive Management Monograph*. Silver Springs, MD: Association of Zoos and Aquariums.
- von Düring, M.** (1973). The ultrastructure of lamellated mechanoreceptors in the skin of reptiles. *Z. Anat. Entwicklungsgesch.* **143**, 81-94.
- von Düring, M.** (1974). The ultrastructure of the cutaneous receptors in the skin of *Caiman crocodilus*. *Abhandlungen Rhein. Westfal. Akad.* **53**, 123-134.
- von Düring, M. and Miller, M. R.** (1979). Sensory nerve endings in the skin and deeper structures. In *Biology of the Reptilia*, Vol. 9, Neurology A (ed. C. Gans, R. G. Northcutt and P. Ulinski), pp. 407-442. New York: Academic Press.
- von Wettstein, O.** (1937). Ordnung der klasse Reptilia: Crocodilia. In *Handbuch der Zoologie eine Naturgeschichte der Stamme Destierreiches* (ed. W. G. Kükenenthal and T. Krumbach), pp. 236-248. Berlin: Walter de Gruyter & Co.
- Weise, K.** (1974). The mechanoreceptive system of prey localization in *Notonecta*. II. The principle of prey location. *J. Comp. Physiol. A* **92**, 317-325.
- Welker, W. I. and Seidenstein, S.** (1959). Somatic sensory representation in the cerebral cortex of the racoon (*Procyon lotor*). *J. Comp. Neurol.* **111**, 469-501.
- Wellnitz, S. A., Lesniak, D. R., Gerling, G. J. and Lumpkin, E. A.** (2010). The regularity of sustained firing reveals two populations of slowly adapting touch receptors in mouse hairy skin. *J. Neurophysiol.* **103**, 3378-3388.